doi:10.1006/jmbi.2000.4158 available online at http://www.idealibrary.com on IDEAL® J. Mol. Biol. (2000) 303, 721–732

JMB

Crystallographic Analysis Reveals Common Modes of Binding of Medium and Long-chain Fatty Acids to Human Serum Albumin

Ananyo A. Bhattacharya, Tim Grüne and Stephen Curry*

Biophysics Section, Blackett Laboratory, Imperial College of Science, Technology and Medicine, London SW7 2BW UK

*Corresponding author

Human serum albumin (HSA) is an abundant plasma protein that is responsible for the transport of fatty acids. HSA also binds and perturbs the pharmacokinetics of a wide range of drug compounds. Binding studies have revealed significant interactions between fatty acid and drug-binding sites on albumin but high-resolution structural information on ligand binding to the protein has been lacking. We report here a crystallographic study of five HSA-fatty acid complexes formed using saturated medium-chain and long-chain fatty acids (C10:0, C12:0, C14:0, C16:0 and C18:0). A total of seven binding sites that are occupied by all medium-chain and long-chain fatty acids have been identified, although medium-chain fatty acids are found to bind at additional sites on the protein, yielding a total of 11 distinct binding locations. Comparison of the different complexes reveals key similarities and significant differences in the modes of binding, and serves to rationalise much of the biochemical data on fatty acid interactions with albumin. The two principal drug-binding sites, in sub-domains IIA and IIIA, are observed to be occupied by fatty acids and one of them (in IIIA) appears to coincide with a high-affinity long-chain fatty acid binding site.

Keywords: crystal structure; fatty acid binding; lipid; human serum albumin

Introduction

Long-chain fatty acids are required for the synthesis of membrane lipids, hormones and second messengers, and serve as an important source of metabolic energy. Fatty acids are stored as triacylglycerols in adipose tissue and released into the circulation where their low aqueous solubilities (typically < 1 μM) are overcome by serum albumin, an abundant plasma protein. Human serum albumin (HSA) greatly enhances the transport capacity of plasma, since it is present at around 0.6 mM and can carry at least six molecules of fatty acid. Under normal physiological conditions, HSA carries around 0.1-2 mol of fatty acid per mol protein (Fredrickson *et al.*, 1958).

HSA is capable of binding an extraordinarily broad range of drugs, and much of the clinical and pharmaceutical interest in the protein derives from its effects on drug pharmacokinetics (Robertson & Brodersen, 1991; Dubois *et al.*, 1993; Jakoby *et al.*, 1995; Vorum & Honoré, 1996; Itoh *et al.*, 1997; Demant & Friche, 1998; Molla *et al.*, 1998). Pioneering work by Sudlow found two primary drug-binding sites on the protein, named sites I and II (Sudlow *et al.*, 1975, 1976). Many subsequent studies have shown that the presence of fatty acids has unpredictable effects on drug binding, and both co-operative and competitive interactions have been observed (Vallner, 1977; Birkett *et al.*, 1978; Wanwimolruk *et al.*, 1983; Ivarsen & Brodersen, 1989; Brodersen *et al.*, 1990; Vorum & Honoré, 1996; Curry *et al.*, 1998).

The binding of fatty acids to serum albumin has been studied for over 40 years (Carter & Ho, 1994; Peters, 1995) but our understanding of these interactions is far from complete. Although it is now well established that the protein has multiple fatty acid binding sites of varying affinities (Kragh-Hansen, 1990; Carter & Ho, 1994; Peters, 1995), the

Present address: T. Grüne, EMBL Grenoble Outstation, 6 rue Jules Horowitz, BP156, F-38042 Grenoble Cedex 9, France.

Abbreviations used: HSA, human serum albumin; BSA, bovine serum albumin.

E-mail address of the corresponding author: s.curry@ic.ac.uk

precise number of binding sites is not known; a current consensus seems to be that there are two or three high-affinity sites on the protein and at least three further sites of lower affinity (Carter & Ho, 1994; Peters, 1995). A variety of biochemical and biophysical methods have been used to investigate the nature and locations of fatty acid binding sites and many significant insights have accrued. The mixed electrostatic and hydrophobic nature of the binding interaction has been characterised (Reynolds *et al.*, 1968; Parks *et al.*, 1983; Cistola *et al.*, 1987b) and it has been shown that at several binding sites the carboxylate head-group of the bound fatty acid is more rigidly anchored than the methylene tail (Hamilton *et al.*, 1984). Moreover, the domain locations of some sites have been mapped (Reed *et al.*, 1975; Hamilton *et al.*, 1991), and there are clear indications that the primary sites for medium-chain and long-chain fatty acids are distinct (Means & Bender, 1975; Soltys & Hsia, 1978). However, progress in understanding fatty acid binding has been hampered, due largely to the complexity of the multiple binding interactions but also to the absence of structural information. Almost all of the methods used to identify binding sites have resorted to some form of modification of the protein (Reed *et al.*, 1975; Shaklai *et al.*, 1984; Hamilton *et al.*, 1991) or the ligand (Sklar *et al.*, 1977; Berde *et al.*, 1979; Reed, 1986), which inevitably complicated interpretation of the results. Only recently have structural and mutational approaches been applied to the analysis of ligand binding to HSA.

The first crystallographic analyses of HSA revealed that the protein, a 585 amino acid residue monomer, contains three homologous α-helical domains (I-III) (He & Carter, 1992; Carter & Ho, 1994). The domains each contain ten helices and are divided into six-helix and four-helix sub-domains (A and B); the first four helices of A and B form similar anti-parallel α-helix bundles. These investigations found that drug-binding sites I and II on HSA are located in sub-domains IIA and IIIA, respectively (He & Carter, 1992; Ho *et al.*, 1993). We subsequently reported the crystal structure of HSA complexed with a medium-chain fatty acid (myristic acid, C14:0) (Curry *et al.*, 1998, 1999), which brought to light the precise locations of six fatty acid binding sites. This study also uncovered a previously undetected binding site for drug compounds, immediately adjacent to a bound fatty acid molecule in sub-domain IA (Curry *et al.*, 1998).

However, C14:0 is not found in appreciable quantities circulating in plasma (Saifer & Goldman, 1961) except under certain conditions of disease or clinical treatment (Bach & Babayan, 1982; Babayan, 1987; Bougnères *et al.*, 1989). Therefore, to assess the generality of our findings from the structure of the HSA-C14:0 complex, we have extended our analysis and present the crystal structures of four new HSA-fatty acid complexes. These include complexes with the saturated fatty acids C10:0, C12:0, C16:0 and C18:0 (capric, lauric, palmitic and stearic acid, respectively; in the C*m*:*n* nomenclature adopted for this work, *m* gives the number of carbon atoms in the methylene tail and *n* is the number of double bonds). We have re-refined the structure of the HSA-C14:0 complex using a more complete high-resolution data set than that available previously.

Results

Structure determination

HSA-fatty acid complexes were prepared by incubating the protein with a large molar excess of fatty acid (see Materials and Methods; Table 1). Five different complexes were prepared in the course of the present work using C10:0, C12:0, C14:0, C16:0 and C18:0 fatty acids. The complexes all crystallized isomorphously with HSA-C14:0 (Curry *et al.*, 1998) and the structures were solved by molecular replacement. Difference electron density maps showed clear density for multiple bound fatty acids in each case. At most sites (exceptions are noted below) the shape of the density, which had a significant broadening at one end, clearly indicated the position of the carboxylate moiety and thus defined the orientation of the bound lipid. This usually placed the carboxylate group of the fatty acid adjacent to an amino acid side-chain with which it could make a salt-bridge or hydrogen bond. Models for each HSA-fatty acid complex were constructed and refined to resolutions of 2.44-2.70 Å; the models have R_{free} values in the range 25.8-28.8 % and reasonable stereochemistry (Table 2). While it was not possible at these resolutions to assign the dihedral angles within the methylene tails of the bound fatty acids precisely, the overall shapes of the tails were well-defined. Average *B*-factors for the different models are relatively high, ranging from 52-61 Å^2; sub-domain

Table 1. Summary of co-crystallisation conditions

	Process	C10:0	C12:0	C14:0	C16:0	C18:0
Fatty acid (mM)	Complexing	10	5	2.4	2.5	0.8
HSA:FA molar ratio	Complexing	>40	30	12	20	>20
Fatty acid (mM)	Washing	5.0	0.5	0.1	0.1	0.05
PEG 3350 (%, w/v)	Crystallisation	28	28	28	28	31
PEG 3350 (%, w/v)	Harvest	35	35	35	35	34

Table 2. Data collection and model refinement statistics

HSA-fatty acid complex	C10:0	C12:0	C14:0	C16:0	C18:0
A. *Data collection*					
Unit cell dimensions					
a (Å)	186.78	188.50	191.84	190.09	189.60
b (Å)	39.19	38.90	39.02	38.75	38.84
c (Å)	95.34	95.77	95.88	95.87	95.98
β(deg.)	105.15	104.63	105.12	104.96	105.49
Source[a]	D-9.6	H-X31	D-9.5	H-X31	D-9.6
Resoution range (Å)	37.5-2.5	12.0-2.45	13.0-2.5	12.0-2.44	40.0-2.7
Independent reflections	22984	23657	23210	24122	17689
Multiplicity	3.2	1.5	1.9	2.7	2.5
Completeness (%)[b]	97.5 (100)	92.7(83.6)	96.2(92.4)	92.9(87.8)	93.7(96.8)
$I/\sigma I$	5.3(2.5)	9.5(3.1)	3.7(3.0)	9.4(4.0)	4.5(2.4)
R_{merge} (%)[c]	7.0(27.3)	3.8(22.6)	5.7(22.4)	4.6(17.8)	9.0(24.8)
B. *Model refinement*					
RCSB PBD ID	1e7e	1e7f	1e7g	1e7h	1e7i
Number of non-hydrogen atoms	4561	4478	4598	4554	4639
Number of water molecules	31	26	16	29	26
R_{model} (%)[d]	22.0	22.5	22.5	21.4	20.4
R_{free} (%)[e]	27.1	27.6	28.8	27.2	25.9
r.m.s deviation from ideal bond lengths (Å)	0.006	0.007	0.006	0.006	0.007
r.m.s deviation from ideal angles (deg.)	1.16	1.23	1.10	1.21	1.16
r.m.s. deviation in *B*-factors main/side-chain (Å^2)	1.7/2.6	1.7/2.6	1.7/2.7	1.7/2.7	1.7/2.6

[a] D, Sychrotron Radiation Source, Daresbury, UK; H, DESY, Hamburg, Germany.
[b] Values for the outermost resolution shell are given in parentheses.
[c] $R_{merge} = 100\ \Sigma_h\Sigma_j|I_{hj} - I_h|/\Sigma_h\Sigma_j I_{hj}$, where I_h is the weighted mean intensity of the symmetry-related reflections I_{hj}.
[d] $R_{model} = 100\ \Sigma_{hkl}|F_{obs} - F_{calc}|/\Sigma_{hkl}F_{obs}$, where F_{obs} and F_{calc} are the observed and calculated structure factors, respectively.
[e] R_{free} is the R_{model} calculated using a randomly selected 5% sample of reflection data omitted from the refinement.

IIIB consistently exhibits higher than average *B*-factors (65-80 Å^2).

Overview of fatty acid binding

For the four new HSA-fatty acid complexes in this study, the protein conformations are very similar to the structure of HSA-C14:0, which has been described in detail elsewhere (Curry *et al.*, 1998, 1999). The HSA-fatty acid complexes all display the conformational change from the defatted HSA structure (He & Carter, 1992; Sugio *et al.*, 1999) that was observed previously for HSA-C14:0 (Curry *et al.*, 1998). This conformational change involves substantial rotations of domains I and III relative to the central domain II, and appears to be primarily driven by fatty acid binding to the site located at the juncture of sub-domains IA and IIA.

Our original study on the HSA-C14:0 complex positively identified five binding sites for the fatty acid. These consist of a single site in sub-domain IB, one at the interface between sub-domains IA and IIA, two sites in IIIA (Sudlow's drug-binding site II) and a fifth in IIIB (Figure 1). A sixth C14:0-binding site was suggested, on the basis of fragmentary electron density, to lie at the interface between sub-domains IIA and IIB. The present results show that all six sites identified for C14:0 are occupied by all the fatty acids in our study (C10:0, C12:0, C16:0 and C18:0) (Figure 1). In addition, a seventh site has been identified within the drug-binding cavity of sub-domain IIA (Sudlow's drug-binding site I). Moreover, for medium-chain fatty acids (C10:0 to C14:0), the data indicate the presence of further sites (see below).

Common binding sites for medium and long-chain fatty acids

In the discussion of fatty acid binding sites, we have adopted and extended the site-numbering scheme that was established for HSA-C14:0 (Curry *et al.*, 1998).

Site 1

This site lies in a D-shaped cavity in the centre of the four-helix bundle of sub-domain IB (Figure 2). In comparison to the other major fatty acid binding pockets on HSA, this site is relatively open and accessible to solvent. There is clear electron density for all the medium-chain fatty acids (C10:0-C14:0) in their respective complexes but the density becomes progressively weaker and more broken for longer fatty acids. In the HSA-C18:0 complex, the density for the bound fatty acid is especially weak at this site and the side-chain of Tyr138, which lines the binding cavity and contacts the ligand, also appears disordered. In the absence of fatty acid, Tyr138 stacks with Tyr161 and occludes the binding pocket but upon fatty acid binding at this site, the tyrosine side-chains rotate through about 90° so that their phenyl rings hold the lipid in a hydrophobic clamp (Curry *et al.*, 1999) (Figure 2). The disordering of Tyr138 in the HSA-C18:0 structure is an indication that this site

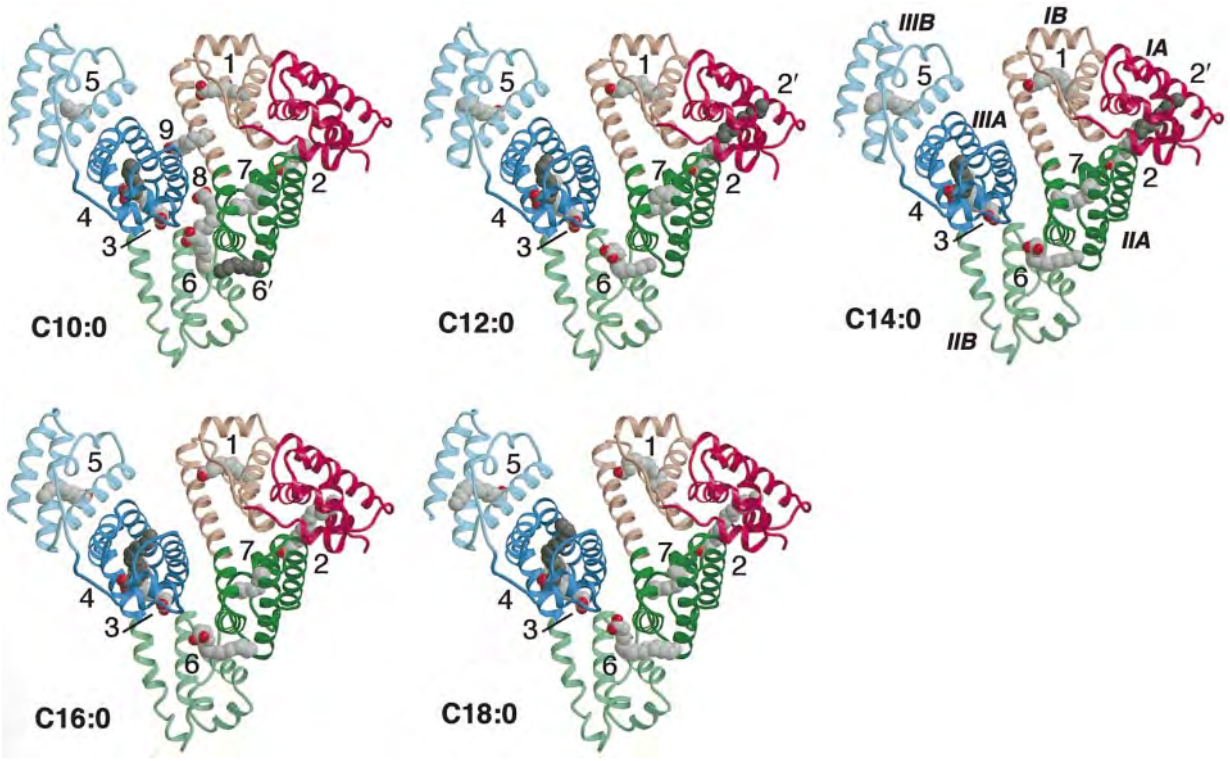

Figure 1. Structures of HSA complexed with five different fatty acids. The protein secondary structure is shown schematically and the domains are colour-coded as follows: I, red; II, green, III, blue. The A and B sub-domains are depicted in dark and light shades, respectively. This colour scheme is maintained throughout. Bound fatty acids are shown in a space-filling representation and coloured by atom type (carbon, grey; oxygen, red). Where two fatty acid molecules bind in close proximity, one of them is shown in a darker shade of grey. All Figures were prepared using Bobscript (Esnouf, 1997) and Raster3D (Merrit & Bacon, 1997).

is not well occupied. The observation that the weakening of the ligand density at site 1 is progressive with increasing chain length for saturated fatty acids suggests that the presumed increase in binding affinity at this site as the ligand becomes longer and more hydrophobic (Ashbrook *et al.*, 1975) does not fully compensate for their lower aqueous solubilities. Although C18:0 may bind to this site at least as tightly as C16:0, its solubility may be too low to allow full occupancy; such ''cut-off'' effects have been observed for the protein binding of other series of aliphatic compounds (Franks & Lieb, 1985; Curry *et al.*, 1990).

All the fatty acids bind at site 1 in the same orientation with the carboxylate group hydrogen-bonded to Arg117 and to a water molecule that is also coordinated by the side-chain hydroxyl group of Tyr161 and the carbonyl oxygen atom of Leu182. For the longer-chain saturated fatty acids, the tail curls around the inside surface of the cavity so that the tip of the hydrophobic tail gradually approaches His146 at the lower end of the cavity opening (Figure 2). This suggests an explanation for the finding that C16:0 and C18:0 but not C8:0 can block the covalent modification of the equivalent His in bovine serum albumin (BSA) by *N*-dansylaziridine (Brown & Shockley, 1982).

Site 2

Located between sub-domains IA and IIA, site 2 is one of the most enclosed fatty acid binding sites on HSA, since even the carboxylate moiety of the ligand is largely shielded from solvent (Figure 3(a)). Binding of fatty acids at this site is implicated in driving the conformational change observed with the uptake of ligand because this site is dislocated into two half-sites in defatted HSA (Curry *et al.*, 1998, 1999); the formation of a contiguous pocket to accommodate the fatty acid requires rotation of domain I relative to domain II and appears to be stabilized by ligand binding. In all cases, the carboxylate head-groups of fatty acids bound to site 2 are anchored in sub-domain IIA by hydrogen bond interactions to the side-chains of Tyr150, Arg257 and Ser287 (Figure 3(a)). The methylene tails extend linearly within the narrow hydrophobic cavity formed by the realignment of IA and IIA; the longest fatty acid tails extend furthest into this cavity. There is good electron density for all the fatty acids (C10:0-C18:0) at this site, indicating that even fatty acids with just ten carbon atoms in the methylene tail are long enough to pin the two half-sites together as a binding pocket. Curiously, we have been unable to co-crystallise HSA with C8:0 in a form that is isomorphous with crystals of the other HSA-fatty acid complexes. Simple modelling

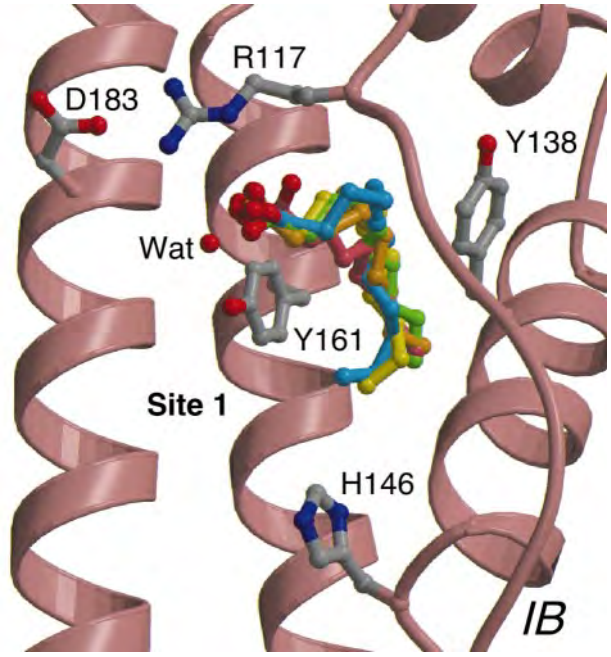

Figure 2. Fatty acid binding to site 1 in sub-domain IB. The protein is coloured as in Figure 1. The fatty acids are coloured using a rainbow scheme: C10:0, red; C12:0, orange; C14:0, yellow; C16:0, green; C18:0, blue (this colour scheme is maintained in subsequent Figures). Selected amino acid side-chains and a bound water molecule are shown coloured by atom type.

experiments suggest that this may be because C8:0 is too short for its methylene tail to make the stabilising contacts with sub-domain IA that are required for the conformational change.

In the case of C12:0, the electron density map showed clear evidence for the presence of a second fatty acid molecule binding in the upper part of the pocket within IA (designated 2′), its tail overlapping in an anti-parallel fashion with the first lipid molecule in site 2 (Figure 3(b)). Examination of a map for the HSA-C14:0 complex calculated from a new high-resolution data set (resolution 2.5 Å, Table 2) confirmed that a second C14:0 molecule was binding at this site, in a configuration essentially identical with that observed for the shorter C12:0 fatty acid. The carboxylate head group for the second molecule, which is not visible in either the HSA-C12:0 or HSA-C14:0 electron density maps, presumably extends into solvent from the upper surface of sub-domain IA and is disordered. In the HSA-C10:0 map, there is only very weak, broken density to suggest the presence of a second fatty acid molecule in site 2. The binding of a second molecule of C10:0 may be much weaker because the methylene tails are too short to allow the overlapping hydrophobic contacts observed for C12:0 and C14:0. For fatty acids longer than C14:0, there is no density at all for a second molecule, perhaps because binding of the first long-chain fatty acid at this site leaves too little room for a second molecule to bind with appreciable affinity.

Sites 3 and 4

Sub-domain IIIA was previously observed to contain two molecules of C14:0, bound at sites 3 and 4 (Curry *et al.*, 1998). The molecules bound approximately at right-angles to one another with their methylene tails in contact (Figures 1 and 4(a)). All the fatty acids included in this study exhibited the same pattern of binding within sub-domain IIIA, sites 3 and 4 both being occupied.

Within site 3, the head-group is fixed in the same position for all fatty acids, by hydrogen bonding to Ser342 and Arg348 from IIB, and Arg485 from IIIA. As the fatty acid tail length increases, the tail is forced into a U-bend configuration, since the longest dimension of the pocket is able to accommodate only about 12-14 methylene

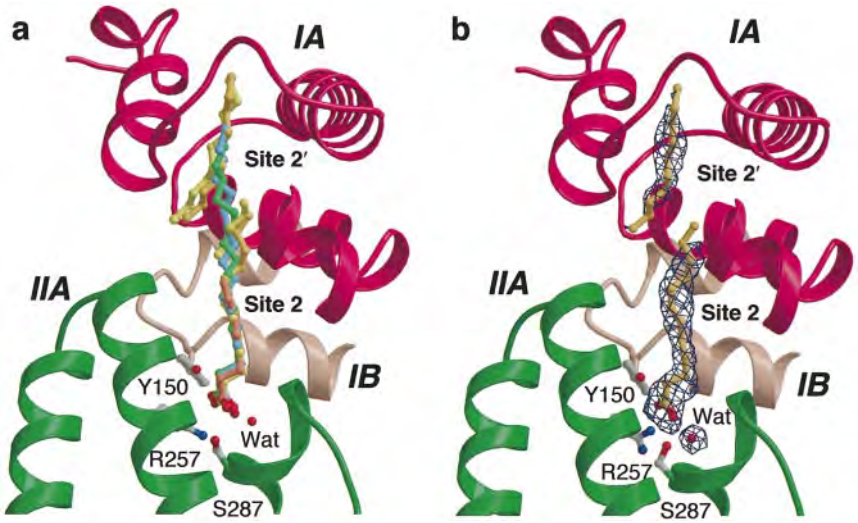

Figure 3. Fatty acid binding to site 2 in sub-domains IA and IIA. (a) Superposition of medium-chain and long-chain fatty acids. (b) Simulated annealing $F_o - F_c$ omit map contoured at 2.75σ, showing difference electron density for C12:0 in site 2. A second molecule is bound in the upper part of the site, designated 2′.

DOCKET ALARM

Explore Litigation Insights

Docket Alarm provides insights to develop a more informed litigation strategy and the peace of mind of knowing you're on top of things.

Real-Time Litigation Alerts

Keep your litigation team up-to-date with **real-time alerts** and advanced team management tools built for the enterprise, all while greatly reducing PACER spend.

Our comprehensive service means we can handle Federal, State, and Administrative courts across the country.

Advanced Docket Research

With over 230 million records, Docket Alarm's cloud-native docket research platform finds what other services can't. Coverage includes Federal, State, plus PTAB, TTAB, ITC and NLRB decisions, all in one place.

Identify arguments that have been successful in the past with full text, pinpoint searching. Link to case law cited within any court document via Fastcase.

Analytics At Your Fingertips

Learn what happened the last time a particular judge, opposing counsel or company faced cases similar to yours.

Advanced out-of-the-box PTAB and TTAB analytics are always at your fingertips.

API

Docket Alarm offers a powerful API (application programming interface) to developers that want to integrate case filings into their apps.

LAW FIRMS
Build custom dashboards for your attorneys and clients with live data direct from the court.

Automate many repetitive legal tasks like conflict checks, document management, and marketing.

FINANCIAL INSTITUTIONS
Litigation and bankruptcy checks for companies and debtors.

E-DISCOVERY AND LEGAL VENDORS
Sync your system to PACER to automate legal marketing.